Physics Procedia

Volume 75, 2015, Pages 995–1002

20th International Conference on Magnetism

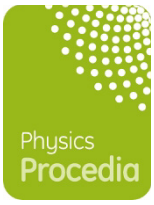

Resonant Magnetoresistance in Asymmetric Double-Barrier Magnetic Tunnel Junctions

Niazbeck Useinov and Lenar Tagirov

Institute of Physics, Kazan Federal University, Kazan, 420008, Russia
Niazbeck.Useinov@kpfu.ru

Abstract

Resonant tunneling is studied theoretically for the planar asymmetrical double-barrier magnetic tunnel junction (DMTJ) when a dc bias field is applied. The spin-polarized conductance and tunnel magnetoresistance (TMR) through the DMTJ have been calculated. In DMTJ nanostructure the magnetization of middle ferromagnetic metal layer can be aligned parallel or antiparallel with respect to the fixed magnetizations of the top and bottom ferromagnetic electrodes. Analytical expression for the transmission coefficient of the DMTJ is received, which is expressed through the single-barrier transmission coefficients taking into account the voltage drop on each barrier and spin degrees of freedom of the electron. The dependencies of the tunnel conductance and TMR on the applied voltage have been calculated for the case of resonant transmission.

Keywords: Spin-polarized conductance, magnetic tunnel junction, nanostructures, tunnel magnetoresistance

1 Introduction

High tunneling magnetoresistance (TMR) effect in magnetic nanostructures, where various ferromagnetic layers are separated by insulators, has attracted considerable interest due to their important applications at room temperatures [1, 2]. The ways to get functionality in nanostructures are to manage transport properties by means of non-uniform magnetism and/or applied voltage. High TMR, desired for magnetic read heads or sensors, is achieved using single MgO barrier, however, it drops steeply with increasing the bias voltage, which limits its application in the high bias-voltage region. Besides single-barrier, the double-barrier MTJs (DMTJs) have also been extensively studied for novel physical phenomena and potential applications in spintronic devices. The DMTJs were studied theoretically and experimentally as well with a special emphasis to quantum well states in the middle metallic layer [4, 7, 8, 9, 10, 11, 12].

Our research is devoted to building of a consecutive theory of TMR adapted to planar asymmetric DMTJs, which have the structure $FM^t/I_1/FM^m/I_2/FM^b$, where FM^t, FM^m and FM^b are the top, middle and bottom ferromagnetic metal layers, while I_1 and I_2 are insulators as

Selection and peer-review under responsibility of the Scientific Programme Committee of ICM 2015

doi:10.1016/j.phpro.2015.12.168

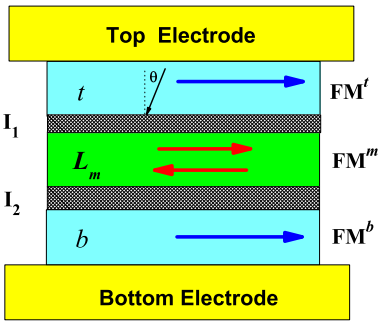

Figure 1: (Color online) Schematic drawing of the cross section of an asymmetric DMTJ. The top (t) and bottom (b) ferromagnetic layers are electrodes of the junction. L_m is the thickness of the middle ferromagnetic layer. The arrows (red and blue) show possible magnetization directions of the ferromagnetic layers. The oblique arrow indicates the direction of the electron conduction trajectory with the incidence angle measured from the z-axis.

shown in Fig. 1. The magnetization direction of the middle layer FM^m can be aligned parallel (P) or antiparallel (AP) with respect to the fixed magnetizations of the top FM^t and bottom FM^b ferromagnetic electrodes. The DMTJ have ferromagnetic layers of thicknesses t, L_m and b, respectively, separated by nonmagnetic insulators of thicknesses t_1 and t_2 of around dozen of angstroms. Typical examples for the constituents of the junction are Co, CoCr, CoFeB, Fe, and NiFe for ferromagnets, and Al_2O_3 and MgO for the insulating nonmagnetic barriers. Note that in this paper we assume FM^m layer having lower coercivity compared with the FM^t and FM^b layers. If voltage is applied to the nanostructure $FM^t/I_1/FM^m/I_2/FM^b$ the spin-polarized tunnel conductance arises. This conductance is induced by quantum tunneling through the barriers. It is very small and decays exponentially with increasing the thickness of the insulators. The FM^m layer can be considered as a quantum well (QW). Then, the motion of electrons in the FM^m layer is quantized. For some parameters of the structure $FM^t/I_1/FM^m/I_2/FM^b$, the resonant conditions can be fulfilled. Then, the spin-polarized tunneling conductance rapidly increases at specific values of the applied voltage. In the resonant tunneling regime transmission coefficients through the double-barrier junction depend on its magnetic configuration and this dependence gives rise to the TMR effect. Original feature of our approach is the self-consistent treatment of dc bias on each barrier, depending on their thickness and dielectric permittivity of the insulators. We assume that electron spin is conserved in the tunneling process through the whole structure and also neglect any spin accumulation. Apart from this we analyze only colinear configurations of the FM magnetizations, which allows us to consider each spin channel separately. Electronic structure of the electrodes is approximated by a free-electron-like dispersion law, which for FM electrodes is spin-split due to an exchange field. We also assume that the barriers are of rectangular shape which transforms into trapezoidal one when a bias voltage V is applied to the DMTJ.

2 Transmission coefficient and resonance condition

As a first step, we derive analytical expressions for the transmission coefficient and the resonance condition in asymmetrical double-barrier structure with QW under a dc bias field. The dc bias field applied to the nanostructure of sandwich type $FM^t/I_1/FM^m/I_2/FM^b$ changes the potential energy landscape and the dispersion laws. The voltage drop on the top insulating layer I_1 and on the bottom insulating layer I_2 are given by the following equations:

$$V_1 = \frac{\varepsilon_2 t_1}{\varepsilon_1 t_2 + \varepsilon_2 t_1} V, \qquad V_2 = \frac{\varepsilon_1 t_2}{\varepsilon_1 t_2 + \varepsilon_2 t_1} V, \tag{1}$$

where V is the total applied voltage, $\varepsilon_{1(2)}$ are the dielectric permittivity of the barriers, respectively.

The coefficient of transmission across the DMTJ can be derived from the electron wave function with standard boundary conditions imposed on the wave function and its first derivative at the each electrode/barrier interface, see for example [10]. When the interfaces are flat, the in-plane component $k^{\parallel}_{t,s}$ of the electron wave vector is conserved in the tunneling processes. Then, the transmission coefficient for an electron incident on the barrier from the top electrode, and with the Fermi energy E_F, measured from the bottom of the electron spin subbands of the top electrode, can be written as a function of the normal component $k_{t,s} = k^t_{F,s}\cos(\theta_{t,s})$ of the electron wave vector. Here the angle $\theta_{t,s}$ is defined by a trajectory of an electron in the top electrode on the direction towards the barrier, see Fig. 1. It is measured from the normal to the contact plane. The absolute value of the Fermi wave vectors $k^t_{F,s}$ corresponds to the spin subband of the electrode FM^t. The index $s = \uparrow, \downarrow$ labels spin states of electrons in $FM^{t(b)}$ and FM^m. After a straightforward algebra, see also [3, 4], we received the transmission coefficient of the asymmetrical DMTJ under the applied voltage:

$$T^{\mathrm{P(AP)}}_{2b,s} = \left[T^{-1}_{1,s}T^{-1}_{2,s} + \left(T^{-1}_{1,s} - 1\right)\left(T^{-1}_{2,s} - 1\right) + \right. \\ \left. +2\sqrt{T^{-1}_{1,s}\left(T^{-1}_{1,s} - 1\right)}\sqrt{T^{-1}_{2,s}\left(T^{-1}_{2,s} - 1\right)}\cos\Phi_{V,s}\right]^{-1}, \tag{2}$$

which is expressed through the single-barrier transmission coefficients

$$T_1 = \frac{4m_1 m_t m_m k_t k_m f_1^2/\pi^2}{(\beta_1 - \gamma_1)^2 + (\chi_1 + \alpha_1)^2}, \qquad T_2 = \frac{4m_2 m_m m_b k_m k_b f_2^2/\pi^2}{(\beta_2 - \gamma_2)^2 + (\chi_2 + \alpha_2)^2}, \tag{3}$$

taking into account the voltage drop on each barrier and spin degrees of freedom of the electron. Here and further, for simplicity, we omit the spin index. In Eq. (2) the characteristic phase difference under the applied bias is $\Phi_V = \phi_1 + \phi_2 + 2k_m L_m$, where ϕ_1 and ϕ_2 are the phase shifts of the electron waves propagation from one barrier to another. These phases are defined by the formulas

$$\phi_1 = \arctan\left[\frac{2(\chi_1\gamma_1 + \beta_1\alpha_1)}{\chi_1^2 - \gamma_1^2 + \beta_1^2 - \alpha_1^2}\right], \qquad \phi_2 = \arctan\left[\frac{2(\chi_2\beta_2 + \gamma_2\alpha_2)}{\beta_2^2 - \chi_2^2 - \gamma_2^2 + \alpha_2^2}\right]. \tag{4}$$

In Eqs. (3), (4) we use the following notation for linear combinations of Airy functions:

$$\begin{aligned}
\alpha_l &= m_l^2 k_{t(m)} k_{m(b)} \left\{ \mathrm{Ai}\left[q_l\left(0\right)\right] \mathrm{Bi}\left[q_l\left(t_l\right)\right] - \mathrm{Bi}\left[q_l\left(0\right)\right] \mathrm{Ai}\left[q_l\left(t_l\right)\right] \right\}, \\
\beta_l &= m_l m_{m(b)} k_{t(m)} f_l \left\{ \mathrm{Ai}\left[q_l\left(0\right)\right] \mathrm{Bi'}\left[q_l\left(t_l\right)\right] - \mathrm{Bi}\left[q_l\left(0\right)\right] \mathrm{Ai'}\left[q_l\left(t_l\right)\right] \right\}, \\
\gamma_l &= m_l m_{t(m)} k_{m(b)} f_l \left\{ \mathrm{Ai'}\left[q_l\left(0\right)\right] \mathrm{Bi}\left[q_l\left(t_l\right)\right] - \mathrm{Bi'}\left[q_l\left(0\right)\right] \mathrm{Ai}\left[q_l\left(t_l\right)\right] \right\}, \\
\chi_l &= m_{t(m)} m_{m(b)} f_l^2 \left\{ \mathrm{Ai'}\left[q_l\left(0\right)\right] \mathrm{Bi'}\left[q_l\left(t_l\right)\right] - \mathrm{Bi'}\left[q_l\left(0\right)\right] \mathrm{Ai'}\left[q_l\left(t_l\right)\right] \right\},
\end{aligned} \tag{5}$$

where $\mathrm{Ai'}\left[q_l\right]$ and $\mathrm{Bi'}\left[q_l\right]$ are the first derivatives of the Airy functions. The arguments $q_l\left(z\right)$ of the Airy functions for our problem can be written as

$$q_l\left(z\right) = f_l \left(z + \frac{\hbar^2 t_l \left(k_F^{t(m)}\right)^2}{2 m_l e V_l} - \frac{t_l \left(E_F + U_l\right)}{e V_l} \right), \tag{6}$$

where the factor f_l here and in Eqs. (3) and (5) have the form $f_l = \left(2 m_l e V_l / \hbar^2 t_l\right)^{1/3}$, for the subscript $l = 1, 2$. The basic mathematical background and the calculation details can be found in article [10].

Next, let us investigate the resonance condition in the model studied here. Because of $0 < T_1 < 1$ and $0 < T_2 < 1$, as seen from Eq. (2), it is understood that $T_{2b}^{\mathrm{P(AP)}}$ shows a local minimum for $\cos\Phi_V = 1$, and a local maximum for $\cos\Phi_V = -1$. Then for $\Phi_V = \phi_1 + \phi_2 + 2k_m L_m = (2n+1)\pi$ $(n = 0, 1, 2, ...)$ we obtain the local maximum value of the transmission coefficient by

$$T_{2b,\max}^{\mathrm{P(AP)}} = \left[\sqrt{T_1^{-1} T_2^{-1}} - \sqrt{\left(T_1^{-1} - 1\right)} \sqrt{\left(T_2^{-1} - 1\right)} \right]^{-2}. \tag{7}$$

Thus, from the above functional dependencies we can calculate, for example, the bottom barrier width t_2 at fixed values of the top barrier width t_1 and the well width L_m by the equation $\Phi_V = \phi_1 + \phi_2 + 2k_m L_m = (2n+1)\pi$, once the desired Fermi wave vectors for electrons of spin subbands, the total applied voltage V are selected, and the values of the barrier heights, U_1 and U_2, and the electron effective masses for all layers are given. Also, we can select at will the voltage at which the unity resonant transmission coefficient can be obtained.

The dependences of a maximum values of the transmission coefficient vs applied bias across the asymmetrical DMTJ for four spin conduction channel are shown in Fig. 2. The curves were calculated by Eq. (7), with the following parameters of the structure: the values of the Fermi wave vectors for electrons of the spin subbands of the FM layers are $k_{F,\uparrow}^t$=1.1 Å^{-1}, $k_{F,\downarrow}^t$=0.98 Å^{-1}, $k_{F,\uparrow}^b$=1.04 Å^{-1}, $k_{F,\downarrow}^b$=0.97 Å^{-1}, and $k_{F,\uparrow}^m$=0.99 Å^{-1}, $k_{F,\downarrow}^m$=0.96 Å^{-1}, respectively. The Fermi energy E_F was determined by the values of wave vectors of the medial FM^m layer. The effective masses of conduction electrons in the ferromagnetic layers correspond to the free electron mass $m_e = m_t = m_m = m_b$. Two dielectric oxide layers have lateral sizes comparable with the mean free path of conduction electrons. The thicknesses were taken t_1=15.0 Å, t_2=19.0 Å, and heights of the energy potentials above the Fermi energy are U_1=0.24 eV, U_2=0.18 eV. It is also assumed that the dielectric constants are ε_1 =10.1, ε_2=9.8 [6]. The effective masses of electrons in the barriers were assumed to be $m_1 = m_2 = 0.4 m_e$. The upward arrow indicates the spin subband of the majority electrons, and the downward arrow

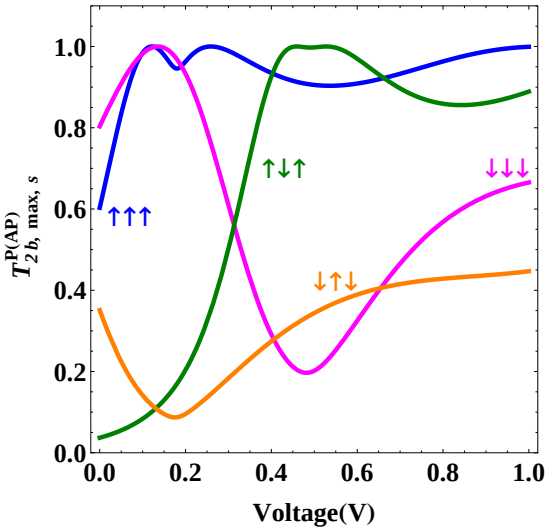

Figure 2: (Color online) Dependences of a maximum value of the transmission coefficient vs applied bias in the asymmetrical DMTJ for four spin conduction channels is denoted by arrows under the resonant conditions, $\cos\Phi_{V,s} = -1$.

indicates the spin subband of the minority electrons. For the P alignment of magnetizations of the top and bottom ferromagnetic electrodes $FM^{t(b)}$, and the middle layer FM^{m}, the electron moves in the following spin subbands: $s =\uparrow (\downarrow)$, $s' =\uparrow (\downarrow)$, $s =\uparrow (\downarrow)$. There are two spin channels of conduction. For the AP alignment the electron moves in the spin subbands $s =\uparrow (\downarrow)$, $s' =\downarrow (\uparrow)$, $s =\uparrow (\downarrow)$. These constitute another two spin channels of conduction.

Five transmission peaks appear in the range 0.0-1.0 V, for different spin conduction channels. The first two peaks show a unity resonance transmission approximately at 0.13 V. Since the eigenenergy levels in an asymmetrical double-barrier magnetic structures move lower under the applied positive voltage, another peak (the third peak) appears for the spin conduction channel (↑↑↑). We recognize at a glance that the third resonant peak in the transmission shows up at 0.25 V, and so on.

3 Spin-polarized conductance

The spin-polarized conductance through the magnetic tunneling nanostructures may be calculated in the frame of the quasi-classical theory [5, 14]. Having found the transmission coefficient one can calculate the spin-polarized conductance through the planar asymmetric DMTJ with the cross-sectional area of the radius a. When a bias voltage V is applied at room temperature it is then given by the formula

$$G_s^{\mathrm{P(AP)}} = G_0 \frac{\left(k_{F,s}^{t(b)} a\right)^2}{2} \left\langle \cos\theta_{t(b),s} T_{2b,s}^{\mathrm{P(AP)}} \left(V, \cos\theta_{t(b),s}\right) \right\rangle, \tag{8}$$

where G_0 is the conductance quantum ($G_0 = 3.87 \times 10^{-5}$ Ohm^{-1}), $T_{2b,s}^{\mathrm{P(AP)}}\left(V, \cos\theta_{t(b),s}\right)$ is the transmission coefficient of an electron as a function of applied voltage and the angle $\theta_{t(b),s}$ of incidence of an electron. The index t or b is selected depending on polarity of the applied

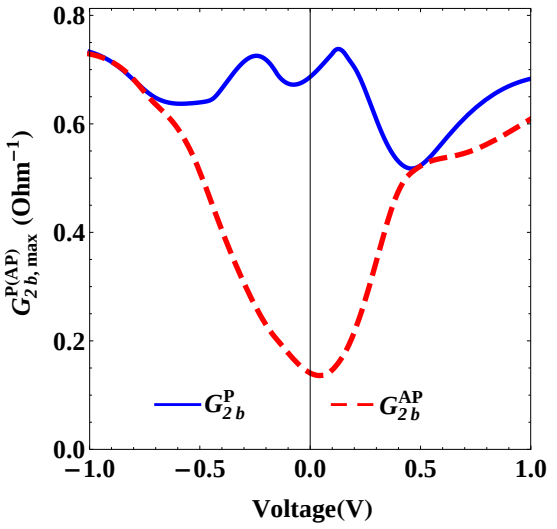

Figure 3: (Color online) The tunnel conductances vs applied bias across the asymmetrical DMTJ in the parallel (solid line) and antiparallel (dashed line) magnetization configurations at room temperature.

voltage V. The angular brackets denote averaging over the angles φ and $\theta_{t(b),s}$. The angle φ lies in the contact plane. The angle $\theta_{t(b),s}$ is defined by a trajectory of an electron in the top or bottom electrodes in the direction to the barrier.

In Fig. 3, dependencies of the tunnel spin-polarized conductance on the applied voltage V are shown for the P and AP alignment of the layer FM^m magnetization with respect to the pinned magnetizations of the top FM^t and bottom FM^b. The $G_{2b}^{\mathrm{P(AP)}}$ are the sums of the spin-up and spin-down conductances $G_{\uparrow}^{\mathrm{P(AP)}}$ and $G_{\downarrow}^{\mathrm{P(AP)}}$. In our numerical calculations we assumed that the cross-sectional area of the structure DMTJ has the radius $a = 20$ nm. The thickness of the middle FM^m layer was taken 25.0 Å. Other parameters used in the calculations correspond to Fig. 2. The bias voltage dependence of the conductance is asymmetric with respect to positive and negative voltages when the magnetic electrodes are not identical and the barriers have different thicknesses. Also the prominent broad valleys in conductance at 0.3 V and 0.7 V are shown for P and AP configuration in DMTJ, respectively. This phenomenon may be attributed to the creation of spin-dependent QW states in the middle FM^m layer, which can lead to discrete energy levels for the majority spins, whereas continuous energy levels for the minority spins are realized [12]. Simultaneously, certain spin channels of conduction may be referred to the consecutive non-resonant tunneling. The predominant elastic tunneling, where incident electrons from one electrode tunnel to the opposite electrode through the double-barrier without loss of energy, gives rise to a significant background to the conductance vs voltage.

4 The tunnel magnetoresistance

The TMR of the DMTJ is defined by the change of the conductance from P to AP alignment of magnetization of the middle ferromagnetic layer FM^m with respect to the fixed magnetizations

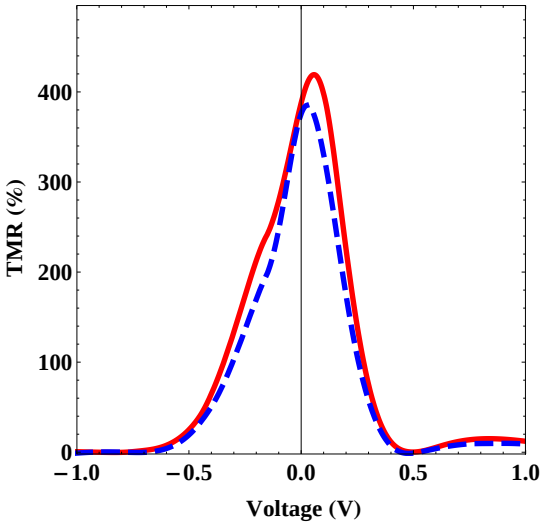

Figure 4: (Color online) TMR in the case of resonant (solid line) and non-resonant (dash line) tunnelling of electrons through the DMTJ. The parameters used in the calculations of the curves correspond to Fig. 3 .

of the top FM^t and bottom FM^b ferromagnetic electrodes. It can be expressed as follows:

$$\mathrm{TMR} = \frac{G_{2b}^{\mathrm{P}} - G_{2b}^{\mathrm{AP}}}{G_{2b}^{\mathrm{AP}}} \cdot 100\%. \tag{9}$$

For the numerical calculation, FM^t, FM^b and FM^m were assumed to be made of different ferromagnetic metals. The two dielectric oxide layers I_1 and I_2 have a lateral size comparable with the mean-free paths of the conduction electrons in the ferromagnetic layers. In Fig. 4 the dependence of TMR on the applied voltage V for the structures $FM^t/I_1/FM^m/I_2/FM^b$ is shown. The solid line corresponds to the resonance conditions, $\cos\Phi_{V,s} = -1$, (formula (7) is used for calculation of the conductance $G_s^{\mathrm{P(AP)}}$) when the tunneling of electrons is combined with the interference of de Broglie waves at the boundaries of the energy barriers for each spin channel of conduction. The dash-line curve was obtained using Eq. (2) for non-resonant conditions.

Finally, we note that although our model does not take into account other complications such as the multiband structure of the ferromagnetic electrodes and the complex band structure of the insulator, or the electron-electron interactions, spin-wave emission and absorption, and inelastic tunneling processes, Coulomb blockade, nevertheless, it provides a reasonable basis for estimation of the spin-dependent tunneling in DMTJs.

Acknowledgments

The reported study was partially supported by RFBR, research project No. 14-02-00348 a, and by the Program of Competitive Growth of Kazan Federal University.

References

[1] Handbook of Magnetism and Advanced Magnetic Materials. Volume 5: Spintronics and Magnetoelectronics, edited by H. Kronmüller and S. Parkin. John Wiley & Sons, Ltd. © 2007.

[2] Edited by E. Tsymbal and I. Žutić. Handbook of Spin Transport and Magnetism. CRC Press Taylor & Francis Group © 2012.

[3] Miyamoto K, Yamamoto H. Resonant tunneling in asymmetrical double-barrier structures under an applied electric field. *J Appl Phys* 1998; **84**: 311-318.

[4] Wilczyński M, Barnas J. Tunnel magnetoresistance in ferromagnetic double-barrier planar junctions: coherent tunneling regime. *J Magn Magn Mater* 2000; **221**: 373-381.

[5] Tagirov LR, Vodopyanov BP, Efetov KB. Ballistic versus diffusive magnetoresistance of a magnetic point contact. *Phys Rev B* 2001; **63**: 104428-4.

[6] Mazierska J, Ledenyov D, Jacob MV, Krupka J. Precise microwave characterization of MgO substrates for HTS circuits with superconducting post dielectric resonator *Supercond.Sci.Technol.* 2005; **18**; 1823.

[7] Peralta-Ramos J, Llois AM, Rungger I, Sanvito S. $I-V$ curves of Fe/MgO (001) single- and double-barrier tunnel junctions. *Phys Rev B* 2008; **78**: 024430-5.

[8] Iovan A, Andersson S, Naidyuk YG, Vedyaev A, Dieny B, Korenivski V. Spin diode based on Fe/MgO double tunnel junction. *Nano Letters* 2008; **8**: 805-809.

[9] Gan HD, Ikeda S, Shiga W, Hayakawa J, Miura K, et al. Tunnel magnetoresistance properties and film structures of double MgO barrier magnetic tunnel junctions. *Appl Phys Lett* 2010; **96**: 192507-3.

[10] Useinov AN, Kosel J, Useinov NK, Tagirov LR. Resonant tunnel magnetoresistance in double-barrier planar magnetic tunnel junctions. *Phys Rev B* 2011; **84**; 085424-8.

[11] Liu R, Yang S.-H, Jiang X, Topuria T, Rice PM, Rettner C, Parkin S. Tunneling magnetoresistance oscillations due to charging effects in MgO double barrier magnetic tunnel junctions. *Appl Phys Lett.* 2012; **100**: 012401-3.

[12] Liu RS, Yang S.-H, Jiang X, Zhang X.-G, Rettner C, et al. CoFe alloy as middle layer for strong spin dependent quantum well resonant tunneling in MgO double barrier magnetic tunnel junctions. *Phys Rev B* 2013; **87**: 024411-5.

[13] Useinov NK, Petukhov DA, Tagirov LR. Tunnel magnetoresistance in asymmetric double-barrier magnetic tunnel junctions. *J Magn Magn Mater* 2015; **373**: 27-29.

[14] Useinov NK. Semiclassical Greens functions of magnetic point contacts. *Theor and Math Phys* 2015; **183**: 705714.